Solid-emissive fluorophores constructed by a non-planar heteropolycyclic structure with bulky substituents: synthesis and X-ray crystal structures†

Yousuke Ooyama, Shintaro Yoshikawa, Shigeru Watanabe and Katsuhira Yoshida*

Received 18th January 2007, Accepted 20th February 2007
First published as an Advance Article on the web 7th March 2007
DOI: 10.1039/b700848a

Novel solid-emissive indeno[1,2-*b*]benzo[4,5-*e*]pyran-11-one-type fluorophores **3a–3c** having non-planar structures with sterically hindered substituents (R = butyl, phenyl, and thienyl) have been designed and conveniently synthesized. The fluorescence quantum yields of **3a–3c** in 1,4-dioxane were **3a** ($\Phi = 0.053$) $\gg$ **3b** ($\Phi = 0.013$) > **3c** ($\Phi = 0.003$). On the other hand, the solid-state fluorescence quantum yields of the fluorophores were **3a** ($\Phi = 0.39$) > **3b** ($\Phi = 0.15$) > **3c** ($\Phi = 0.06$). To elucidate the large differences in the quantum yields in solution and in the solid state and among the fluorophores **3a–3c**, we performed time-resolved fluorescence spectroscopic measurements, semi-empirical molecular orbital calculations (AM1 and INDO/S), and X-ray crystallographic analyses of **3a–3c**. The comparison of the values of the radiative and non-radiative rate constants determined by the time-resolved spectroscopic measurements in solution and in the crystalline state supported that non-radiative decay is reduced by restriction of the rotation of the phenyl and thienyl rings in the solid state. In addition, the X-ray crystal structures demonstrated that, in **3a** and **3b**, the non-planar structure with sterically hindered substituents prevents the fluorophores from forming short π–π contacts and produces strong solid-state fluorescence. On the other hand, in the crystal of **3c**, the formation of continuous intermolecular CH · · · S bonding between neighboring fluorophores was found to increase short π–π contacts and reduce the fluorescence intensity.

Introduction

Solid-state fluorescence of organic fluorophores has recently attracted increasing interest because of their many uses both in the fundamental research field of solid-state photochemistry[1] and in the applied field of optoelectronic devices.[2] However, organic fluorophores with strong solid-emissive properties are rare, because most organic fluorophores undergo fluorescence quenching in molecular aggregation states. Many efforts have been carried out to avoid the concentration quenching. For example, Chen *et al.* have recently reported the strong solid-state fluorescence of diphenylfumaronitrile derivatives having non-planar structures which inhibit the close packing of the molecules that causes fluorescence quenching.[1e] On the other hand, Tohnai *et al.*[1h] proposed the possibility of a tunable solid-state fluorescence system consisting of an organic salt with a primary amine. In the system, the fluorescence intensity can be controlled by changing the alkyl chain length of the amine. In contrast, Yoshida *et al.*[3] reported that quinol-type fluorophores exhibit significant changes of color and a drastic fluorescence enhancement upon inclusion of guest molecules in the crystalline state. From the relation between the solid-state fluorescence properties and the crystal structures, it was confirmed that the destruction of π–π interactions between the fluorophores by guest enclathration is the main reason for the guest-dependent fluorescence enhancement behavior. Strong intermolecular π–π interactions[1c–g,3–5] or continuous intermolecular hydrogen bonding[3b,6] between neighboring fluorophores have been suggested as main factors of fluorescence quenching. Ultimately, the key point in the design of strong solid-emissive fluorophores is to eliminate the factors that induce concentration quenching in molecular aggregation states.

In this paper, we report a molecular design and the convenient synthesis of novel solid-emissive indeno[1,2-*b*]benzo[4,5-*e*]pyran-11-one-type fluorophores (**3a–3c**)[7] constructed with a non-planar structure with sterically hindered substituents. To elucidate the differences between the photophysical properties in solution and in the solid state, we have performed time-resolved fluorescence spectroscopic measurements, semi-empirical molecular orbital calculations (AM1 and INDO/S), and X-ray crystallographic analyses of **3a–3c**. The relations between the observed photophysical properties and the chemical and crystal structures of the fluorophores are discussed.

Results and discussion

Synthesis of indeno[1,2-*b*]benzo[4,5-*e*]pyran-11-one-type fluorophores by a photochemical rearrangement reaction

The synthetic pathway is shown in Scheme 1. We used 3-(dibutylamino)-6-hydroxy-6-phenyl-naphtho[2,3-*b*]benzofuran-11(6*H*)-one **1**[3a] as a starting material. The reaction of **1** with organolithium reagents gave **2a–2c** in 60–70% yields. The structures of **2a–2c** were confirmed by X-ray diffraction analysis (see ESI†). The proposed reaction mechanism is depicted in Scheme 2: the 1,2-addition of organolithium reagents (RLi) to **1** forms diol derivative **I** and subsequently the rearrangement of the

Department of Material Science, Faculty of Science, Kochi University, Akebono-cho, Kochi, 780-8520, Japan. E-mail: kyoshida@cc.kochi-u.ac.jp; Fax: +81-88844-8359

† Electronic supplementary information (ESI) available: X-ray crystallographic data. See DOI: 10.1039/b700848a

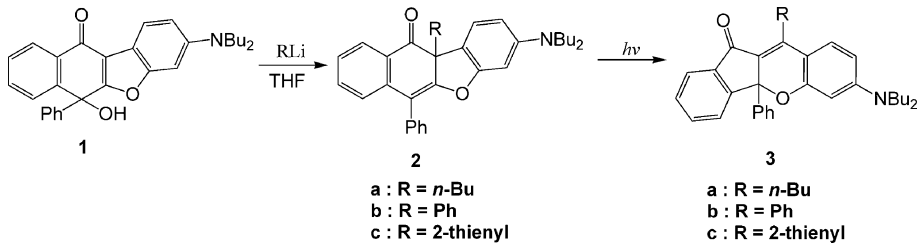

Scheme 1 Outline of the synthetic pathway.

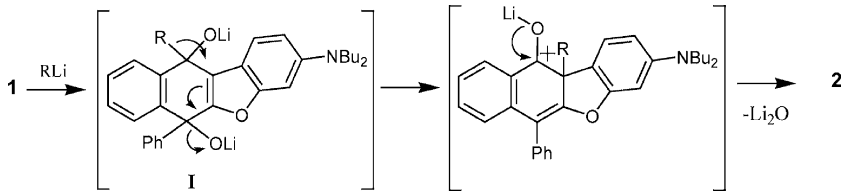

Scheme 2 Proposed mechanism for the reaction of **1** with RLi.

substituent (R) occurs to give the cyclohexadienone-type products **2**. It is known that 1,4-disubstituented cyclohexa-2,5-diene-1,4-diol derivatives undergo acid-promoted dehydration which is followed by rearrangement to produce cyclohexadienone-type compounds.[8,9] Next, the conversion of **2a–2c** to novel heteropolycyclic fluorophores **3a–3c** was performed in 90–100% yields by a photochemical rearrangement reaction, which is a new photoreaction we have found in this research. A possible mechanism for the formation of **3a–3c** from **2** is shown in Scheme 3, which is similar to a photoinduced oxa-di-π-methane rearrangement:[10,11] first, the 1,2-diradical would be derived to form a 1,4-diradical intermediate **II** with a cyclopropane ring. Rearrangement of the intermediate **II** would form a 1,3-diradical intermediate which would then undergo cyclization to give the stable product, indeno[1,2-*b*]benzo[4,5-*e*]pyran-11-one **3**. As a typical example, Fig. 1 shows (a) the absorption and (b) the fluorescence spectral changes obtained by irradiation of **2b** in 1,4-dioxane at 365 nm with a black light. Upon irradiation, a new intense absorption band appeared at around 455 nm together with isosbestic points 325 and 363 nm, and the corresponding fluorescence band appeared at 520 nm. The appearance of the strong absorption and fluorescence bands in the visible region is ascribed to extension of π-conjugation by the photochemical rearrangement.

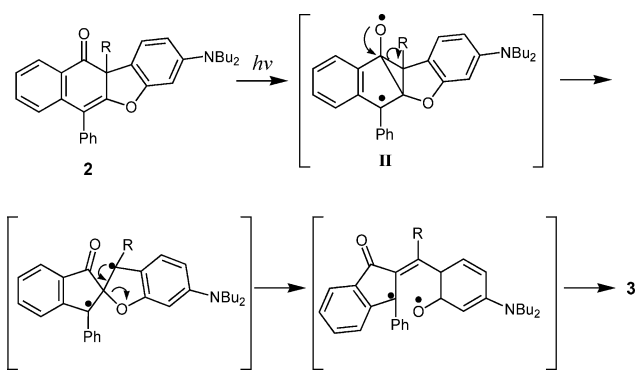

Scheme 3 Proposed mechanism for the photoarrangement of **2** to **3**.

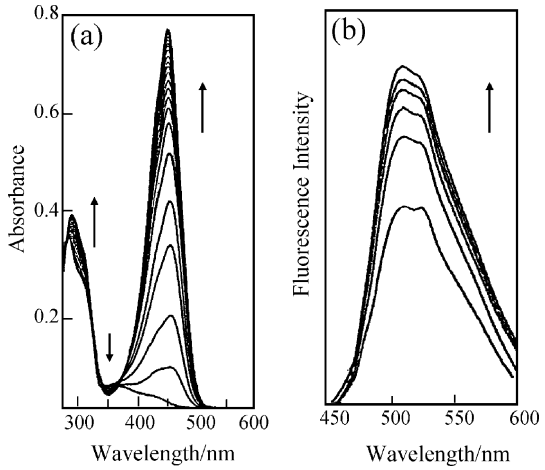

Fig. 1 (a) Absorption and (b) fluorescence spectral changes upon photoirradiation of **2b** in benzene. [**2b**] = 2.5×10^{-5} M.

Spectroscopic properties of indeno[1,2-*b*]benzo[4,5-*e*]pyran-11-one-type fluorophores in solution and in the solid state

The fluorescence spectra of **3a–3c** in 1,4-dioxane and in the crystalline state were recorded by excitation at the wavelength of the longest absorption maximum. Fig. 2 and Table 1 show the spectroscopic properties of **3a–3c** in 1,4-dioxane. The absorption maxima at around 447–460 nm and the fluorescence maxima at around 497–532 nm are both red-shifted by conjugation with the substituent (R) in the order of **3a** < **3b** < **3c** (Fig. 2). On the other hand, the fluorescence intensity decreases dramatically in the order of **3a** ($\Phi_f = 0.053$) ≫ **3b** ($\Phi_f = 0.013$) > **3c** ($\Phi_f = 0.003$). The time-resolved fluorescence spectroscopy of **3a–3c** indicated that the relatively high fluorescence quantum yield of **3a** is mainly due to a large radiative rate constant ($k_r = 8.28 \times 10^7$ s^{-1}) compared to those of the other compounds **3b** ($k_r = 1.29 \times 10^7$ s^{-1}) and **3c** ($k_r = 0.05 \times 10^7$ s^{-1}). The ratio of non-radiative constant to radiative constant (k_{nr}/k_r) increases in the order of **3a** (17.8) < **3b** (75.7) < **3c** (364), which is compatible with the order of fluorescence quantum yield of **3a–3c**. These results suggest that non-radiative decay is

Table 1 Spectroscopic properties of **3a–3c** in 1,4-dioxane

	λ_{max}^{abs}/nm[a] (ε_{max}/dm^3 mol^{-1} cm^{-1})	λ_{max}^{fl}/nm[b]	Φ_f[c]	τ[d]/ns	k_r[e]/10^7 s^{-1}	k_{nr}[f]/10^7 s^{-1}
3a	447(32300)	497	0.053	0.64	8.28	148
3b	455(30500)	519	0.013	1.01	1.29	97.7
3c	460(28600)	532	0.003	5.47	0.05	18.2

[a] 1.25×10^{-5} M. [b] 1.25×10^{-6} M. [c] Φ_f values were determined using 9,10-bisphenylethynylanthracene ($\Phi_f = 0.84$, $\lambda_{ex} = 440$ nm) in benzene as a standard. [d] Fluorescence lifetime. [e] Radiative rate constant ($k_r = \Phi_f/\tau_f$). [f] Non-radiative rate constant ($k_{nr} = (1 - \Phi_f)/\tau_f$).

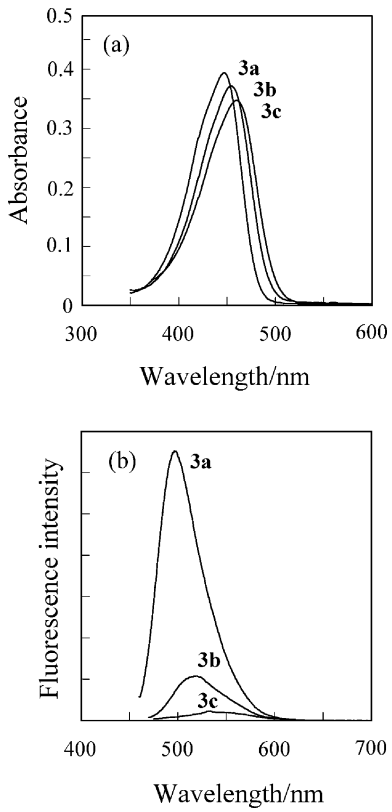

Fig. 2 (a) Absorption and (b) fluorescence spectra of compounds **3a–3c** in 1,4-dioxane.

accelerated by free rotation of the phenyl ring and thienyl ring in solution.

Of particular interest are the solid-state photophysical properties. Fig. 3 and Table 2 show the spectroscopic properties of **3a–3c** in the crystalline state. The fluorescence quantum yields of **3a–3c** are in the order of **3a** ($\Phi_f = 0.39$) > **3b** ($\Phi_f = 0.15$) > **3c** ($\Phi_f = 0.06$) in the crystalline state. The fluorophors **3a–3c** exhibited much stronger fluorescence in the solid state than in solution. Since the rotation of the substituents is restricted in the solid state, the fluorescence quantum yields are higher in the solid state than in solution. The longest wavelengths of the absorption and fluorescence maxima of **3a–3c** are red-shifted in the order of **3a** ≈ **3b** < **3c** in comparison with those of **3a–3c** in 1,4-dioxane. The time-resolved fluorescence spectroscopy of **3a–3c** indicates that the fluorescence quantum yield depends on the ratio of radiative rate constant to non-radiative rate constant: (k_r/k_{nr}) = **3a** (0.64) > **3b** (0.18) > **3c** (0.06). From the lower quantum yields of **3c** both in solution and in the solid state, it was considered that strong electron-donating effect of the thienyl group caused not

Table 2 Spectroscopic properties of **3a–3c** in the crystalline state

	λ_{max}^{ex}/nm	λ_{max}^{fl}/nm	Φ_f[a]	τ[b]/ns	k_r[c]/10^8 s^{-1}	k_{nr}[d]/10^8 s^{-1}
3a	485	522	0.39	1.08	3.61	5.65
3b	495	531	0.15	0.93	1.61	9.14
3c	537	567	0.06	0.59	1.02	15.9

[a] The solid fluorescence quantum yields (Φ_f) were determined by using a calibrated integrating sphere system ($\lambda_{ex} = 325$ nm). [b] Fluorescence lifetime. [c] Radiative rate constant ($k_r = \Phi_f/\tau_f$). [d] Nonradiative rate constant ($k_{nr} = (1 - \Phi_f)/\tau_f$).

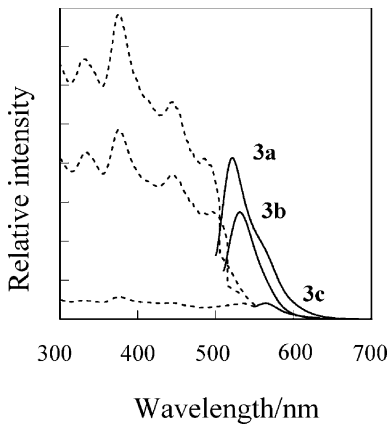

Fig. 3 Solid-state excitation (dotted line) and emission (solid line) spectra of the crystals of **3a–3c**.

only the red-shift of the absorption and fluorescence maxima but also significant fluorescence quenching.

Semi-empirical MO calculations (AM1, INDO/S)

The absorption spectra of **3a–3c** were analyzed by using semi-empirical molecular orbital (MO) calculations. The molecular structures were optimized by using the MOPAC/AM1 method,[12] and then the INDO/S method[13] was used for spectroscopic calculations. The calculated absorption wavelengths and the transition character of the first absorption bands are collected with those of the observed spectra (Table 3). As shown in Fig. 4, the optimized geometries of **3a–3c** show that the heteropolycyclic skeleton is non-planar because of the existence of the central sp^3 carbon where the phenyl group is attached. Moreover, it was found that the phenyl and thienyl substituents of **3b** and **3c** are able to rotate freely compared to the butyl substituent of **3a**, which is compatible with the observed fluorescence properties in 1,4-dioxane. The values of the dipole moments in the ground states are 6.18 for **3a**, 6.13 for **3b**, and 4.81 for **3c** and the differences between the dipole moments ($\Delta\mu$) of the first excited and the ground states

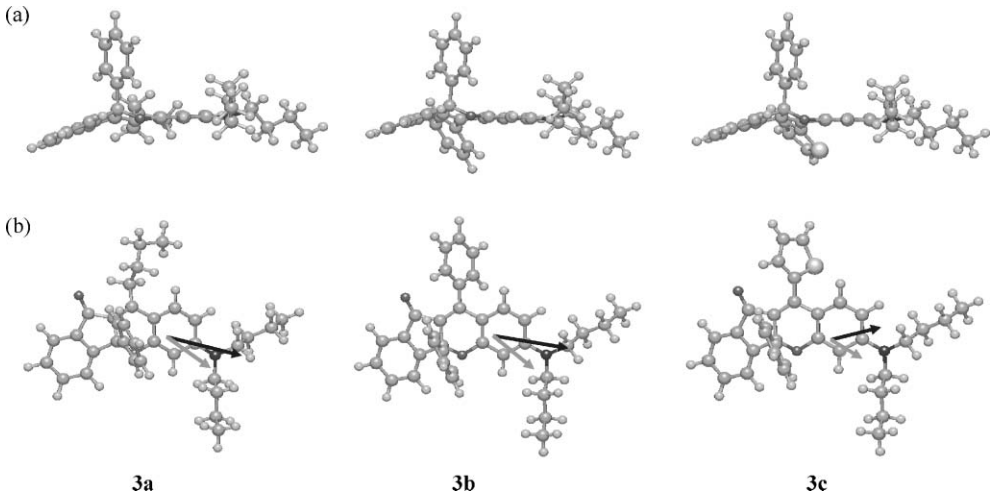

Fig. 4 The optimized geometries of **3a–3c** by using the MOPAC/AM1 method: (a) side view, and (b) top view with the dipole moments in the ground states (gray) and the difference dipole moments between the excited and the ground states (black).

Table 3 Calculated absorption spectra for the compounds **3a–3c**

		Absorption (calc.)			
Quinol	μ/D[a]	λ_{max}/nm	f[b]	CI component[c]	$\Delta\mu$/D[d]
3a	6.18	353	0.68	HOMO → LUMO (85%)	8.53
3b	6.13	362	0.61	HOMO → LUMO (87%)	8.42
3c	4.81	372	0.50	HOMO → LUMO (74%)	5.80

[a] The values of the dipole moment in the ground state. [b] Oscillator strength. [c] The transition is shown by an arrow from one orbital to another, followed by its percentage CI (configuration interaction) component. [d] The values of the difference in the dipole moment between the excited and the ground states.

are 8.53 for **3a**, 8.42 for **3b**, and 5.80 for **3c**. The values of the dipole moments of **3c** are small compared to those of **3a** and **3b**. As shown also in Fig. 4(b), although the directions of the dipole moment of **3a–3c** in the ground state are similar, the direction of the dipole moment of **3c** in the excited state is different from those of **3a** and **3b**. These results suggested that the thienyl group as electron donor contributes significantly to the π-conjugated system of the fluorophore, which affects the photophysical properties of **3c**.

The calculated absorption wavelengths and the oscillator strength values are compatible with the observed spectra in 1,4-dioxane, although the calculated absorption spectra are blue shifted. This deviation of the INDO/S calculations, giving high transition energies compared with the experimental values, has been generally observed.[14] The calculations show that the longest excitation bands for **3a–3c** are mainly assigned to the transition from the HOMO to the LUMO, where the HOMO is mostly localized on the dibutylaminobenzopyran moiety, and the LUMO is mostly localized on the indenone moiety. However, the HOMO of **3c** is also localized on the thienyl ring. The changes in the calculated electron density accompanying the first electron excitation are shown in Fig. 5, which shows a strong migration of intramolecular charge-transfer character of **3a–3c**. It is noteworthy that the thienyl group of **3c** as electron donor is taking part in the intramolecular charge transfer, but the butyl group of **3a** and the phenyl group of **3b** are not. These results indicates that electron-donating effects of the π-conjugated thienyl group on the intramolecular charge transfer cause red shifts of the absorption and fluorescence maxima and significant fluorescence quenching both in solution and in the solid state.

X-Ray crystal structures of indeno[1,2-*b*]benzo[4,5-*e*]pyran-11-one-type fluorophores

In order to investigate the effect of the crystal structure on the solid-state photophysical properties, we have performed X-ray crystallographic analyses of **3a–3c**. The crystal systems

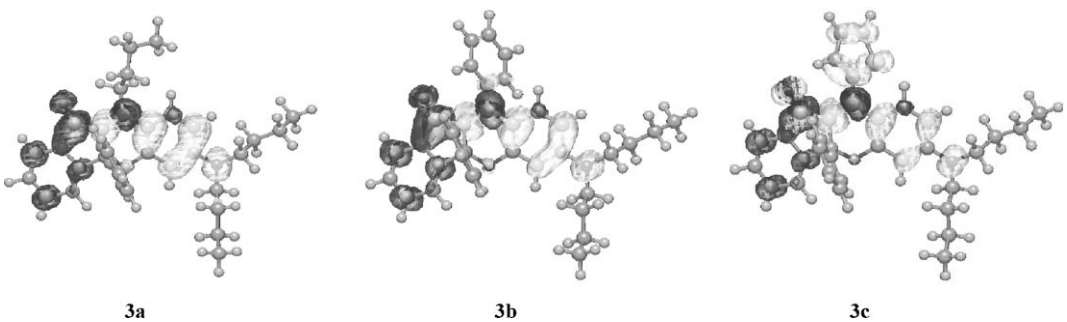

Fig. 5 Calculated electron density changes accompanying the first electronic excitation of **3a–3c**. The white and black lobes signify decreases and increases in electron density accompanying the electronic transition. Their areas indicate the magnitude of the electron density change.

were monoclinic with space group $P2_1/c$ with $Z = 4$ for **3a**, orthorhombic with space group *Pbca* with $Z = 8$ for **3b**, and triclinic with space group $P\bar{1}$ with $Z = 2$ for **3c**. The packing structures demonstrate that the molecules are arranged in a "herring-bone" fashion in the crystal of **3a**, and in a "bricks in a wall" fashion in the crystals of **3b** and **3c**. As shown in Fig. 6–8, the three crystals are built up by a centrosymmetric pair unit of two enantiomers. Fig. 9 shows the schematic structure of one of the enantiomers. The heteropolycyclic skeleton is non-planar because of the existence of the central sp^3 carbon where the phenyl group is attached. Good correlations were observed between the bond lengths and bond angles of **3a–3c** from semi-empirical MO calculations and those experimentally obtained from X-ray crystal structures. We expected that such non-planar structures with sterically hindered substituents (the phenyl, R, and 7-dibutylamino groups) prevent the fluorophores from forming short π–π contacts causing fluorescence quenching in the solid state. In fact, the torsion angles between the indenone skeleton and the benzopyran skeleton of **3a–3c** are near 150.2°, 150.1°, and 153.1°, respectively. The compounds **3a** and **3b** which exhibit strong solid-state fluorescence have only one or two interatomic contacts of less than 3.60 Å between the neighboring fluorophores in the crystal structure (Fig. 6 and 7). On the other hand, compound **3c** which exhibits unexpected weak solid-state fluorescence has 15 interatomic contacts of less than 3.60 Å between the neighboring fluorophores (Fig. 8(d)). As shown in Fig. 8(b), the fluorophores are linked continuously by intermolecular CH···S bonds between the adjoining benzene ring and thienyl ring of neighboring fluorophores. Thus, the formation of continuous molecular linking by CH···S bonds enables fluorophore **3c** to form such a massed molecular packing structure.

Conclusions

Novel heteropolycyclic fluorophores (**3a–3c**) have been designed and conveniently synthesized by a new photochemical rearrangement reaction that we have found. The X-ray crystal structure analysis demonstrated that, in the crystals of **3a** and **3b**, the non-planar structure with sterically hindered substituents prevents the fluorophores from forming short intermolecular contacts and produces intense solid-state fluorescence emission. However, in the crystal of **3c**, the formation of continuous intermolecular CH···S bonding between the adjoining benzene ring and thienyl ring of neighboring fluorophores increases short π–π contacts and reduce the fluorescence intensity. Thus, new useful information concerning the solid-state fluorescence has been obtained.

Experimental

Melting points were measured with a Yanaco micro melting point apparatus MP-500D. IR spectra were recorded on a JASCO FT/IR-5300 spectrophotometer for samples in KBr pellet form. Absorption spectra were observed with a JASCO U-best30 spectrophotometer and fluorescence spectra were measured with a JASCO FP-777 spectrophotometer. Single-crystal X-ray diffraction was performed on a Rigaku AFC7S diffractometer. Photoirradiation was carried out by using a UVP Model UVGL-25 as the light source. Fluorescence lifetimes were determined with a time-resolved spectrophotometer. The samples were exited by a laser diode ($\lambda_{ex} = 375$ nm). The fluorescence quantum yields (Φ_f) were determined using 9,10-bisphenylethynylanthracene ($\Phi_f = 0.84$, $\lambda_{ex} = 440$ nm)[15] in benzene as the standard. The solid-fluorescence quantum yields (Φ_f) were determined by using a

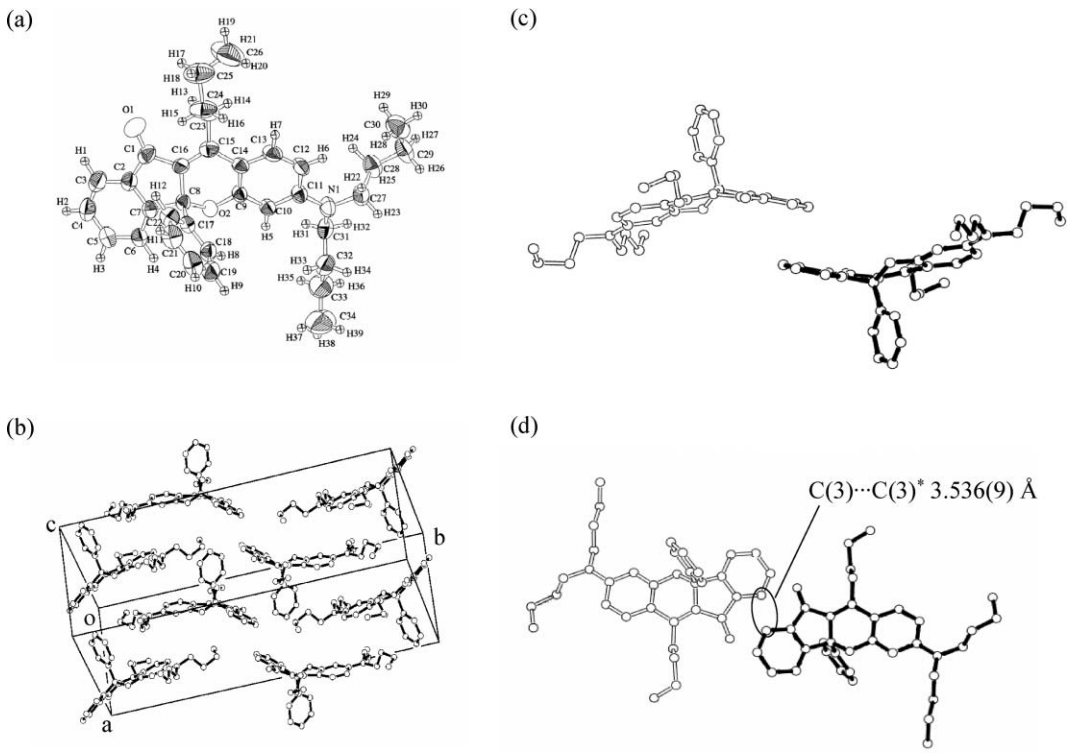

Fig. 6 Crystal packing of **3a**: (a) ORTEP diagram, (b) view of the molecular packing structure, (c) side view, and (d) top view of the pairs of fluorophores.

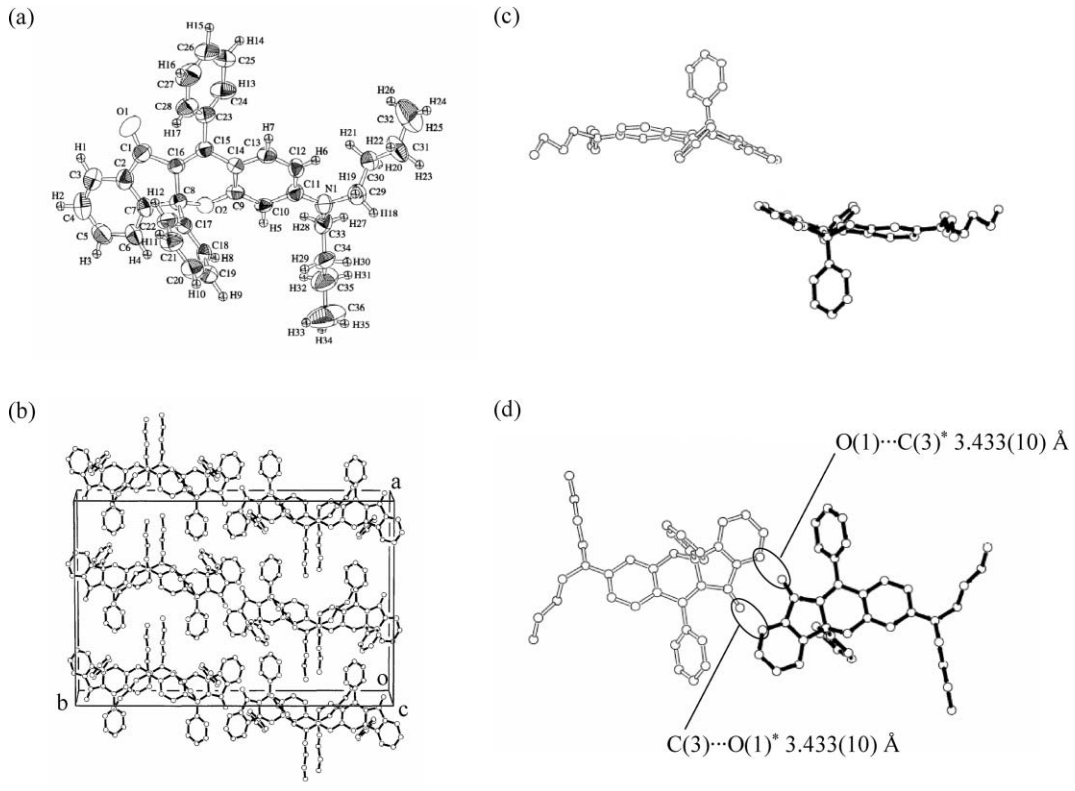

Fig. 7 Crystal packing of **3b**: (a) ORTEP diagram, (b) view of the molecular packing structure, (c) side view, and (d) top view of the pairs of fluorophores.

calibrated integrating sphere system (λ_{ex} = 325 nm). Elemental analyses were recorded on a Perkin Elmer 2400 II CHN analyzer. ^{1}H NMR spectra were recorded on a JNM-LA-400 (400 MHz) FT NMR spectrometer with tetramethylsilane (TMS) as an internal standard. Column chromatography was performed on silica gel (60N, spherical, neutral).

Synthesis of 11a-butyl-3-dibutylamino-6-phenyl-11a*H*-benzo[*b*]naphtho[2,3-*d*]furan-11-one (2a)

To a THF solution (200 ml) of benzofuranoquinol **1** (1.0 g, 2.20 mmol) in Ar atmosphere was added an ethereal solution of 1.6 M butyllithium (5.5 ml, 8.8 mmol) at −108 °C over 30 min. After stirring for 30 min at room temperature, the reaction was quenched with saturated NH_4Cl solution. The solvent was evaporated and the residue was extracted with CH_2Cl_2. The organic extract was washed with water. The organic extract was evaporated and the residue was chromatographed on silica gel (CH_2Cl_2 as eluent) to give **2a** (0.75 g, yield 69%): mp 141–143 °C; FTIR (KBr)/cm^{-1} 1692; ^{1}H NMR (400 MHz, acetone-d_6) δ = 0.77 (3H, t), 0.93 (6H, t), 1.15–1.20 (2H, m), 1.33–1.44 (6H, m), 1.53–1.60 (4H, m), 1.83–1.90 (2H, m), 3.32 (4H, m), 6.29 (1H, d, J = 2.44 Hz), 6.44 (1H, dd, J = 2.44 and 8.54 Hz), 7.08 (1H, d, J = 7.81 Hz), 7.33–7.37 (1H, m), 7.42–7.44 (5H, m), 7.49–7.57 (2H, m), 7.90 (1H, dd, J = 1.46 and 7.56 Hz); ^{13}C NMR (400 MHz, acetone-d_6) δ = 14.1, 14.2, 20.8, 23.0, 27.3, 42.8, 51.5, 61.0, 94.3, 107.11, 111.6, 112.7, 126.7, 126.8, 127.2, 127.8, 128.5, 128.8, 129.4, 131.3, 134.9, 135.3, 140.8, 150.5, 160.6, 162.0, 200.2. Found: C, 83.02; H, 8.26; N, 2.89. $C_{34}H_{39}NO_2$ requires C, 82.72; H, 7.96; N, 2.84%.

Synthesis of 3-dibutylamino-6,11a-diphenyl-11a*H*-benzo[*b*]naphtho[2,3-*d*]furan-11-one (2b)

To a THF solution (100 ml) of benzofuranoquinol **1** (1.0 g, 2.20 mmol) in Ar atmosphere was added an ethereal solution of 1.8 M phenyllithium (4.9 ml, 8.8 mmol) at −108 °C over 30 min. After stirring for 30 min at room temperature, the reaction was quenched with saturated NH_4Cl solution. The solvent was evaporated and the residue was extracted with CH_2Cl_2. The organic extract was washed with water. The organic extract was evaporated and the residue was chromatographed on silica gel (CH_2Cl_2 as eluent) to give **2b** (0.84 g, yield 68%): mp 159–160 °C; FTIR (KBr)/cm^{-1} 1693; ^{1}H NMR (400 MHz, acetone-d_6) δ = 0.91 (6H, t), 1.28–1.38 (4H, m), 1.48–1.56 (4H, m), 3.22–3.34 (4H, m), 6.25 (1H, d, J = 2.44 Hz), 6.41 (1H, dd, J = 2.44 and 8.54 Hz), 7.05 (1H, d, J = 7.56 Hz), 7.19–7.33 (4H, m), 7.45–7.51 (2H, m), 7.55–7.59 (4H, m), 7.67–7.71 (3H, m), 7.76 (1H, dd, J = 1.46 and 7.56 Hz); ^{13}C NMR (400 MHz, acetone-d_6) δ = 14.2, 20.8, 51.5, 64.4, 94.4, 107.3, 114.5, 114.6, 126.1, 127.0, 127.6, 128.1, 128.8, 129.5, 129.6, 130.0, 131.3, 134.9, 135.1, 140.5, 140.9, 150.5, 158.8, 160.1, 198.3. Found: C, 84.34; H, 6.92; N, 2.60. $C_{36}H_{35}NO_2$ requires: C, 84.18; H, 6.87; N, 2.73%.

Synthesis of 3-dibutylamino-6-phenyl-11a-thiophen-2-yl-11a*H*-benzo[*b*]naphtho[2,3-*d*]furan-11-one (2c)

To a THF solution (100 ml) of benzofuranoquinol **1** (1.0 g, 2.20 mmol) in Ar atmosphere was added an ethereal solution of 1.0 M 2-thienyllithium (8.8 ml, 8.8 mmol) at −108 °C over 30 min. After stirring for 30 min at room temperature, the reaction

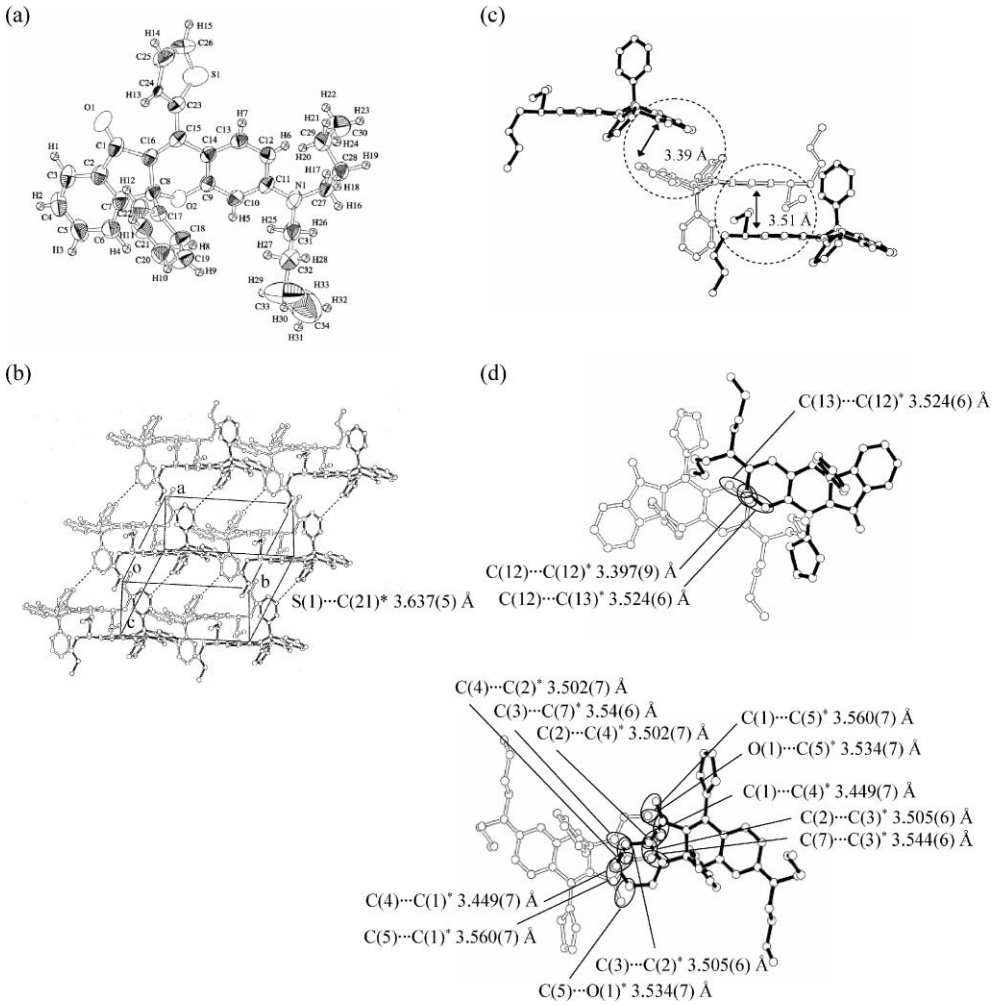

Fig. 8 Crystal packing of **3c**: (a) ORTEP diagram, (b) view of the molecular packing structure, (c) side view, and (d) top views of the pairs of fluorophores.

was quenched with saturated NH_4Cl solution. The solvent was evaporated and the residue was extracted with CH_2Cl_2. The organic extract was washed with water. The organic extract was evaporated and the residue was chromatographed on silica gel (CH_2Cl_2 as eluent) to give **2c** (0.77 g, yield 68%): mp 132–134 °C; FTIR (KBr)/cm^{-1} 1699; ^{1}H NMR (400 MHz, acetone-d_6) δ = 0.92 (6H, t), 1.30–1.39 (4H, m), 1.51–1.58 (4H, m), 3.31 (4H, t), 6.27 (1H, d, J = 2.44 Hz), 6.46 (1H, dd, J = 2.44 and 8.54 Hz), 6.86–6.87 (1H, m), 7.06–7.08 (1H, m), 7.13–7.14 (1H, m), 7.25–7.27 (1H, m), 7.29–7.33 (1H, m), 7.46–7.58 (6H, m), 7.71 (1H, d, J = 8.54 Hz), 7.82 (1H, dd, J = 0.98 and 7.56 Hz); ^{13}C NMR (400 MHz, acetone-d_6) δ = 14.2, 20.8, 51.5, 60.9, 94.3, 107.4, 113.8, 113.8, 125.8, 126.1, 127.0, 127.1, 127.8, 127.9, 128.5, 128.9, 129.0, 129.5, 121.2, 134.9, 135.2, 140.6, 144.9, 150.8, 159.3, 160.2, 196.6. Found: C, 78.61; H, 6.39; N, 2.81. $C_{34}H_{33}NO_2S$ requires: C, 78.58; H, 6.40; N, 2.70%.

Synthesis of 10-butyl-7-dibutylamino-9b-phenyl-9b*H*-indeno[1,2-*b*]benzo[4,5-*e*]pyran-11-one (3a)

A dichloromethane solution (80 ml) of **2a** (0.1 g) was irradiated with 365 nm light. The solvent was evaporated and the residue was purified by silica gel column chromatography (CH_2Cl_2 as eluent) and by recrystallization from a mixture of dichloromethane–*n*-hexane (1 : 1) to give 0.099 g of **3a** in 99% yield as orange crystals: mp 120–122 °C; FTIR (KBr)/cm^{-1} 1679; ^{1}H NMR (400 MHz, acetone-d_6) δ = 0.95–1.00 (9H, m), 1.35–1.51 (6H, m), 1.58–1.65 (4H, m), 2.04–2.09 (2H, m), 3.19–3.23 (2H, m), 3.39–3.43 (4H, m), 6.37 (1H, dd, J = 2.44 and 8.78 Hz), 6.53 (1H, d, J = 2.44 Hz), 7.11–7.15 (1H, m), 7.21–7.25 (2H, m), 7.34 (1H, d, J = 8.78 Hz), 7.48–7.56 (3H, m), 7.60–7.63 (1H, m), 7.71–7.77 (2H, m); ^{13}C NMR (400 MHz, acetone-d_6) δ = 14.2, 14.3, 20.8, 23.5, 27.3, 33.3, 51.2, 82.5, 100.4, 107.3, 113.1, 123.7, 125.4, 126.2, 126.7, 128.2, 129.0, 129.2, 130.1, 134.8, 140.2, 144.8, 146.6, 152.3, 152.4, 158.8, 189.2. Found: C, 82.43; H, 8.25; N, 2.68. $C_{34}H_{39}NO_2$ requires C, 82.72; H, 7.96; N, 2.84%.

Synthesis of 7-dibutylamino-9b,10-diphenyl-9b*H*-indeno[1,2-*b*]benzo[4,5-*e*]pyran-11-one (3b)

A dichloromethane solution (80 ml) of **2b** (0.1 g) was irradiated with 365 nm light. The solvent was evaporated and the residue was purified by silica gel column chromatography (CH_2Cl_2 as eluent) and by recrystallization from a mixture of dichloromethane–*n*-hexane (1 : 1) to give 0.098 g of **3b** in 98% yield as orange crystals: mp 157–159 °C; FTIR (KBr)/cm^{-1} 1686; ^{1}H NMR (400 MHz,

acetone-d_6) δ = 0.96 (6H, t), 1.36–1.45 (4H, m), 1.59–1.66 (4H, m), 3.40–3.44 (4H, m), 6.30 (1H, dd, J = 2.44 and 8.78 Hz), 6.61 (1H, d, J = 2.44 Hz), 6.72 (1H, d, J = 8.78 Hz), 7.16–7.20 (1H, m), 7.28–7.31 (2H, m), 7.47–7.50 (5H, m), 7.62–7.68 (3H, m), 7.73–7.78 (3H, m); ^{13}C NMR (400 MHz, acetone-d_6) δ = 14.2, 20.8, 51.2, 83.1, 100.3, 107.2, 113.6, 113.7, 123.6, 125.5, 126.4, 128.2, 128.4, 129.2, 129.9, 130.2, 131.9, 134.9, 140.3, 144.3, 144.6, 152.2, 152.5, 159.3, 187.1. Found: C, 84.34; H, 6.92; N, 2.60. $C_{36}H_{35}NO_2$ requires C, 84.18; H, 6.87; N, 2.73%.

Synthesis of 10-(2-thienyl)–7-dibutylamino-9b-phenyl-9b*H*-indeno[1,2-*b*]benzo[4,5-*e*]pyran-11-one (3c)

A dichloromethane solution (80 ml) of **2c** (0.1 g) was irradiated with 365 nm light. The solvent was evaporated and the residue was purified by silica gel column chromatography (CH_2Cl_2 as eluent) and by recrystallization from a mixture of dichloromethane–*n*-hexane (1 : 1) to give 0.099 g of **3c** in 99% yield as orange crystals: mp 129–131 °C; FTIR (KBr)/cm^{-1} 1680; ^{1}H NMR (400 MHz, acetone-d_6) δ = 0.98 (6H, t), 1.36–1.46 (4H, m), 1.60–1.67 (4H, m), 3.43 (4H, t), 6.35 (1H, d, J = 2.68 and 8.78 Hz), 6.60 (1H, d, J = 2.68 Hz), 7.11 (1H, d, J = 9.21 Hz), 7.16–7.19 (1H, m), 7.24–7.30 (3H, m), 7.48–7.52 (1H, m), 7.62–7.72 (6H, m), 7.75–7.77 (1H, m); ^{13}C NMR (400 MHz, acetone-d_6) δ = 14.2, 20.8, 51.2, 83.4, 100.3, 107.2, 113.4, 113.5, 123.7, 125.5, 126.4, 127.5, 128.5, 129.2, 129.7, 130.3, 132.0, 133.6, 134.9, 135.1, 136.7, 130.3, 144.2, 151.9, 152.7, 159.2, 186.6. Found: C, 78.56; H, 6.49; N, 2.82. $C_{34}H_{33}NO_2S$ requires C, 78.58; H, 6.40; N, 2.70%.

X-Ray crystallographic studies[7]

The data sets were collected at 23 ± 1 °C on a Rigaku AFC7S four-circle diffractometer by the 2θ–ω scan technique, and using graphite-monochromated Mo-Kα (λ = 0.71069 Å) radiation at 50 kV and 30 mA. In all case, the data were corrected for Lorentz and polarization effects. A correction for secondary extinction was applied. Crystal data, data collection and refinement parameters are summarized in ESI† Table S1. A correction for secondary extinction was supplied. The reflection intensities were monitored by three standard reflections for every 150 reflections. An empirical absorption correction based on azimuthal scans of several reflections was applied. All calculations were performed using the teXsan[16] crystallographic software package of Molecular Structure Corporation.

Crystal structure determination of compound 2a

Crystals of **2a** were recrystallized from a mixture of dichloromethane and *n*-hexane as air stable yellow prisms. The one selected had approximate dimensions 0.40 × 0.40 × 0.50 mm. The transmission factors ranged from 0.86 to 0.99. The crystal structure was solved by direct methods using SIR 92.[17] The structures were expanded using Fourier techniques.[18] The non-hydrogen atoms were refined anisotropically. Some hydrogen atoms were refined isotropically, the rest were fixed geometrically and not refined.

Crystal data. $C_{34}H_{39}NO_2$, M = 493.69, monoclinic, a = 14.321(2), b = 11.583(3), c = 17.877(2) Å, β = 104.490(8)°, U = 2871.3(9) Å^3, T = 296.2 K, space group $P2_1/n$ (no. 14), Z = 4, μ(Mo-K$_\alpha$) = 0.70 cm^{-1}, 5552 reflections measured, 5047 unique (R_{int} = 0.042) which were used in all calculations. The final R indices were $R1$ = 0.074, wR (F^2) = 0.183 (all data).

Crystal structure determination of compound 2b

Crystals of guest-free **2b** were recrystallized from a mixture of dichloromethane and *n*-hexane as air stable yellow prisms. The one selected had approximate dimensions 0.70 × 0.10 × 0.40 mm. The transmission factors ranged from 0.96 to 1.00. The crystal structure was solved by direct methods using SIR 92.[17] The structures were expanded using Fourier techniques.[18] The non-hydrogen atoms were refined anisotropically. Some hydrogen atoms were refined isotropically, the rest were fixed geometrically and not refined.

Crystal data. $C_{36}H_{35}NO_2$, M = 513.68, monoclinic, a = 9.081(2), b = 20.626(4), c = 15.600(3) Å, β = 98.69(2)°, U = 2888(1) Å^3, T = 296.2 K, space group $P2_1/c$ (no. 14), Z = 4, μ(Mo-K$_\alpha$) = 0.72 cm^{-1}, 5427 reflections measured, 5087 unique (R_{int} = 0.059) which were used in all calculations. The final R indices were $R1$ = 0.055, wR (F^2) = 0.174 (all data).

Crystal structure determination of compound 2c

Crystals of **2c** were recrystallized from a mixture of dichloromethane and *n*-hexane as air stable yellow prisms. The one selected had approximate dimensions 0.60 × 0.50 × 0.10 mm. The transmission factors ranged from 0.87 to 1.00. The crystal structure was solved by direct methods using SIR 92.[17] The structures were expanded using Fourier techniques.[18] The non-hydrogen atoms were refined anisotropically. Some hydrogen atoms were refined isotropically, the rest were fixed geometrically and not refined.

Crystal data. $C_{34}H_{33}NO_2S$, M = 519.70, triclinic, a = 10.088(8), b = 16.317(6), c = 9.031(6) Å, α = 91.18(4)°, β = 97.28(6)°, γ = 72.73(4)°, U = 1407(1) Å^3, T = 296.2 K, space group $P\bar{1}$ (no. 2), Z = 2, μ(Mo-K$_\alpha$) = 1.46 cm^{-1}, 6872 reflections measured, 6463 unique (R_{int} = 0.084) which were used in all calculations. The final R indices were $R1$ = 0.094, wR (F^2) = 0.194 (all data).

Crystal structure determination of compound 3a

Crystals of **3a** were recrystallized from a mixture of dichloromethane and *n*-hexane as air stable orange prisms. The one selected had approximate dimensions 0.20 × 0.20 × 0.40 mm. The transmission factors ranged from 0.97 to 1.00. The crystal structure was solved by direct methods using SIR 92.[17] The structures were expanded using Fourier techniques.[18] The non-hydrogen atoms were refined anisotropically. Some hydrogen atoms were refined isotropically, the rest were fixed geometrically and not refined.

Crystal data. $C_{34}H_{39}NO_2$, M = 493.69, monoclinic, a = 9.471(5), b = 30.489(6), c = 10.734(5) Å, β = 114.03(3)°, U = 2830(2) Å^3, T = 296.2 K, space group $P2_1/a$ (no. 14), Z = 4, μ(Mo-K$_\alpha$) = 0.71 cm^{-1}, 5417 reflections measured, 4981 unique (R_{int} = 0.050) which were used in all calculations. The final R indices were $R1$ = 0.053, wR (F^2) = 0.117 (all data).

Crystal structure determination of compound 3b

Crystals of **3b** were recrystallized from a mixture of dichloromethane and *n*-hexane as air stable orange prisms. The one selected had approximate dimensions 0.20 × 0.10 × 0.45 mm. The transmission factors ranged from 0.95 to 1.00. The crystal structure was solved by direct methods using SAPI91.[19] The structures were expanded using Fourier techniques.[18] The non-hydrogen atoms were refined anisotropically. Some hydrogen atoms were refined isotropically, the rest were fixed geometrically and not refined.

Crystal data. $C_{36}H_{35}NO_2$, $M = 513.68$, orthorhombic, $a = 20.947(7)$, $b = 31.759(7)$, $c = 8.758(7)$ Å, $U = 5826(4)$ Å^3, T = 296.2 K, space group *Pbca* (no. 61), $Z = 8$, μ(Mo-K$_\alpha$) = 0.71 cm^{-1}, 5385 reflections measured, 4786 unique ($R_{int} = 0.000$) which were used in all calculations. The final R indices were $R1 = 0.055$, $wR(F^2) = 0.108$ (all data).

Crystal structure determination of compound 3c

Crystals of **3c** were recrystallized from a mixture of dichloromethane and *n*-hexane as air stable orange prisms. The one selected had approximate dimensions 0.50 × 0.40 × 0.40 mm. The transmission factors ranged from 0.87 to 1.00. The crystal structure was solved by direct methods using SIR 92.[17] The structures were expanded using Fourier techniques.[18] The non-hydrogen atoms were refined anisotropically. Some hydrogen atoms were refined isotropically, the rest were fixed geometrically and not refined.

Crystal data. $C_{34}H_{33}NO_2S$, $M = 519.70$, triclinic, $a = 11.009(2)$, $b = 13.949(5)$, $c = 9.752(2)$ Å, $\alpha = 97.99(2)°$, $\beta = 101.46(2)°$, $\gamma = 72.82(2)°$, $U = 1397.1(6)$ Å^3, $T = 296.2$ K, space group $P\bar{1}$ (no. 2), $Z = 2$, μ(Mo-K$_\alpha$) = 1.47 cm^{-1}, 6801 reflections measured, 6426 unique ($R_{int} = 0.040$) which were used in all calculations. The final R indices were $R1 = 0.0793$, wR (F^2) = 0.184 (all data).

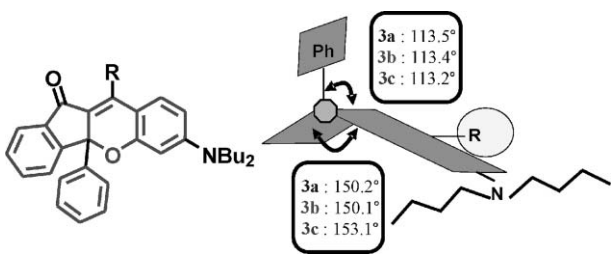

Fig. 9 Schematic representation of the molecular structures of **3a–3c**.

Computational methods

All calculations were performed on a FUJITSU FMV-ME4/657. The semi-empirical calculations were carried out with the Win-MOPAC Ver. 3 package (Fujitsu, Chiba, Japan). Geometry calculations in the ground state were carried out using the AM1 method.[12] All geometries were completely optimized (keyword PRECISE) by the eigenvector following routine (keyword EF). Experimental absorption spectra of the seven quinol derivatives were studied with the semi-empirical method INDO/S (intermediate neglect of differential overlap/spectroscopic).[13] All INDO/S calculations were performed using single excitation full SCF/CI (self-consistent field/configuration interaction), which includes the configuration with one electron excited from any occupied orbital to any unoccupied orbital, 225 configurations were considered for the configuration interaction [keyword CI (15 15)].

Acknowledgements

This work was partially supported by a Grant-in-Aid for Science and Research from the Ministry of Education, Science, Sport and Culture of Japan (Grant 18350100), by a Science and Technology Incubation Program in Advanced Regions of Japan Science and Technology Agency (JST), and by a Special Research Grant for Green Science from Kochi University.

References

1 (*a*) K. Hirano, S. Minakata and M. Komatsu, *Chem. Lett.*, 2001, 8; (*b*) Y. Sonoda, Y. Kawanishi, T. Ikeda, M. Goto, S. Hayashi, N. Tanigaki and K. Yase, *J. Phys. Chem. B*, 2003, **107**, 3376; (*c*) R. Davis, S. Abraham, N. P. Rath and S. Das, *New J. Chem.*, 2004, **28**, 1368; (*d*) V. de Halleux, J.-P. Calbert, P. Brocorens, J. Cornil, J.-P. Declercq, J.-L. Brédas and Y. Geerts, *Adv. Funct. Mater.*, 2004, **14**, 649; (*e*) H.-C. Yeh, W.-C. Wu, Y.-S. Wen, D.-C. Dai, J.-K. Wang and C.-T. Chen, *J. Org. Chem.*, 2004, **69**, 6455; (*f*) E. Horiguchi, S. Matsumoto, K. Funabiki and M. Matsui, *Bull. Chem. Soc. Jpn.*, 2005, **78**, 1167; (*g*) S. Mizukami, H. Houjou, K. Sugaya, E. Koyama, H. Tokuhisa, T. Sasaki and M. Kanesato, *Chem. Mater.*, 2005, **17**, 50; (*h*) Y. Mizobe, N. Tohnai, M. Miyata and Y. Hasegawa, *Chem. Commun.*, 2005, 1839; (*i*) I. Vayá, M. C. Jiménez and M. Miranda, *Tetrahedron: Asymmetry*, 2005, **16**, 2167; (*j*) Z. Xie, B. Yang, L. Liu, M. Li, D. Lin, Y. Ma, G. Cheng and S. Liu, *J. Phys. Org. Chem.*, 2005, **18**, 962; (*k*) A. Dreuw, J. Plötner, L. Lorenz, J. Wachtveitl, J. E. Djanhan, J. Brüning, T. Metz, M. Bolte and M. U. Schmidt, *Angew. Chem.*, 2005, **117**, 7961–7964, (*Angew. Chem., Int. Ed.*., 2005, **44**, 7783–7786).

2 (*a*) C. W. Tang and S. A. VansSlyke, *Appl. Phys. Lett.*, 1987, **51**, 913; (*b*) C. W. Tang, S. A. VansSlyke and C. H. Chen, *J. Appl. Phys.*, 1989, **65**, 3610; (*c*) J. Schi and C. W. Tang, *Appl. Phys. Lett.*, 1997, **70**, 1665; (*d*) A. Kraft, A. C. Grimsdale and A. B. Holmes, *Angew. Chem., Int. Ed.*, 1998, **37**, 402; (*e*) U. Mitschke and P. Bäuerle, *J. Mater. Chem.*, 2000, **10**, 1471; (*f*) K.-C. Wong, Y.-Y. Chien, R.-T. Chen, C.-F. Wang, Y.-T. Liu, H.-H. Chiang, P.-Y. Hsieh, C.-C. Wu, C. H. Chou, Y. O. Su, G.-H. Lee and S.-M. Peng, *J. Am. Chem. Soc.*, 2002, **124**, 11576; (*g*) C. J. Tonzola, M. M. Alam, W. K. Kaminsky and S. A. Jenekhe, *J. Am. Chem. Soc.*, 2003, **125**, 13548; (*h*) H.-C. Yeh, L.-H. Chan, W.-C. Wu and C.-T. Chen, *J. Mater. Chem.*, 2004, **14**, 1293; (*i*) C.-T. Chen, *Chem. Mater.*, 2004, **16**, 4389; (*j*) C.-L. Chiang, M.-F. Wu, D.-C. Dai, Y.-S. Wen, J.-K. Wang and C.-T. Chen, *Adv. Funct. Mater.*, 2005, **15**, 231.

3 (*a*) K. Yoshida, Y. Ooyama, M. Miyazaki and S. Watanabe, *J. Chem. Soc., Perkin Trans. 2*, 2002, 700–707; (*b*) Y. Ooyama, T. Nakamura and K. Yoshida, *New J. Chem.*, 2005, **29**, 447; (*c*) Y. Ooyama, T. Okamoto, T. Yamaguchi, T. Suzuki, A. Hayashi and K. Yoshida, *Chem.–Eur. J.*, 2006, 7827–7838.

4 (*a*) K. Yoshida, J. Yamazaki, Y. Tagashira and S. Watanabe, *Chem. Lett.*, 1996, 9; (*b*) K. Yoshida, T. Tachikawa, J. Yamasaki, S. Watanabe and S. Tokita, *Chem. Lett.*, 1996, 1027; (*c*) K. Yoshida, H. Miyazaki, Y. Miura, Y. Ooyama and S. Watanabe, *Chem. Lett.*, 1999, 837; (*d*) K. Yoshida, Y. Ooyama, S. Tanikawa and S. Watanabe, *Chem. Lett.*, 2000, 714; (*e*) K. Yoshida, Y. Ooyama, S. Tanikawa and S. Watanabe, *J. Chem. Soc., Perkin Trans. 2*, 2002, 708–714; (*f*) Y. Ooyama and K. Yoshida, *New J. Chem.*, 2005, **29**, 1204.

5 H. Langhals, T. Potrawa, H. Nöth and G. Linti, *Angew. Chem.*, 1989, **101**, 497–499, (*Angew. Chem., Int. Ed.*, 1989, **28**, 478–480).

6 K. Yoshida, K. Uwada, H. Kumaoka, L. Bu and S. Watanabe, *Chem. Lett.*, 2001, 808.

7 Y. Ooyama, S. Yoshikawa, S. Watanabe and K. Yoshida, *Org. Biomol. Chem.*, 2006, **4**, 3406–3409.

8 (*a*) H. M. Crowford, M. Lumpkin and M. McDonald, *J. Am. Chem. Soc.*, 1952, **74**, 4087; (*b*) A. Rieker and G. Henes, *Tetrahedron Lett.*, 1968, **34**, 3775–3778; (*c*) F. Alonso and M. Yus, *Tetrahedron*, 1992, **48**, 2709.
9 N. Vorontsova, V. Rozenberg, E. Vorontsov, D. Antonov and Z. Starikova, *Eur. J. Org. Chem.*, 2003, 761–770.
10 (*a*) H. Z. Zimmerman and D. Amresto, *Chem. Rev.*, 1996, **96**, 3065; (*b*) *CRC Handbook of Organic Photochemistry and Photobiology*, ed. W. Horspool and F. Lenci, CRC, New York, 2nd edn, 2004.
11 (*a*) T.-H. Lee, P. D. Rao and C.-C. Liao, *Chem. Commun.*, 1999, 801; (*b*) D. Armesto, M. J. Oritz, A. R. Agarrabeitia and N. El-Boulifi, *Angew. Chem., Int. Ed.*, 2005, **44**, 7739; (*c*) S.-Y. Chang, S.-L. Huang, N. R. Villarante and C.-C. Liao, *Eur. J. Org. Chem.*, 2006, 4648.
12 M. J. S. Dewar, E. G. Zoebisch, E. F. Healy and J. J. Stewart, *J. Am. Chem. Soc.*, 1985, **107**, 389.
13 (*a*) J. E. Ridley and M. C. Zerner, *Theor. Chim. Acta*, 1973, **32**, 111; (*b*) J. E. Ridley and M. C. Zerner, *Theor. Chim. Acta*, 1976, **42**, 223; (*c*) A. D. Bacon and M. C. Zerner, *Theor. Chim. Acta*, 1979, **53**, 21.
14 (*a*) M. Adachi, Y. Murata and S. Nakamura, *J. Org. Chem.*, 1993, **58**, 5238; (*b*) W. M. F. Fabian, S. Schuppler and O. S. Wolfbesis, *J. Chem. Soc., Perkin Trans. 2*, 1996, 853.
15 C. A. Heller, R. A. Henry, B. A. Mclaughlin and D. E. Bills, *J. Chem. Eng. Data*, 1974, **19**, 214.
16 teXsan, Crystal Structure Analysis Package, Molecular Structure Corporation, 1985 and 1992.
17 A. Altomare, M. C. Burla, M. Camalli, M. Cascarano, C. Giacovazzo, A. Guagliardi and G. Polidori, *J. Appl. Crystallogr.*, 1994, **27**, 435.
18 *DIRDIF94*, P. T. Beurskens, G. Admiraal, G. Beurskens, W. P. Bosman, R. de Gelder, R. Israel, J. M. M. Smits, The DIRIF94 program system, Technical Report of the Crystallography Laboratory, University of Nijmegen, The Netherlands, 1994.
19 F. Hai-Fu, *Structure Analysis Programs with Intelligent Control*, Rigaku Corporation, Tokyo, Japan, 1991.